ADULT TISSUE STEM CELLS IN CONTEXT OF HOMEOSTASIS AND TUMOR GROWTH

Schober group at NYU Langone, Ronald O. Perelman Department of Dermatology

Marie-Christin Leitner

University of Vienna

Table of Contents

Introduction

This project was part of a bigger project that led to a paper that is currently submitted (November 2018). This means that all data shown in this report are confidential.

In this report I focused just on work that I performed during my stay at NYU Langone in the Schober group at the Ronald O. Perelman Institute for Dermatology, not the whole paper with the work also performed by others, as they are entitled to take credit for their own work.

I want to thank all my supervisors and mentors, starting with Dr. Markus Schober for accepting me in his lab and giving me the resources do this research. A very special Thank you I want to give to Ana Sastre-Perona PhD, as she taught me everything about this topic and was the best mentor I could ever ask for. Her enthusiasm about this topic is contagious and makes you achieve set goals together as a team.Her effort she put in this paper is outstanding and she is, and will be a great role model and inspiration for me in the future. I also want to thank her and Steven Hoang-Phou for being the best labmates and by now friends that I could ask for.

Furthermore, I want to thank my internal supervisor Dr. Martin Leeb from the University of Vienna for his assistance with the application and his support throughout and after my stay.

Last but not least, I want to thank the Austrian Marshallplan Foundation for their generous support with a scholarship, that made this whole experience possible for me. Without them this research stay abroad would not have been feasible financially. They gave me a great opportunity to broaden my knowledge about science and a field of research that will show promising results in the future. Further they also also gave me the chance to grow as a person with this stay.

The skin and Squamous cell carcinoma

The normal skin, Self-renewal and tumor organization

The epidermis is the barrier to the outer environment and provides the outermost layer of the body. Cells responsible for this function are keratinocytes that form a stratified keratinized epithelium. Other cell types can be found in de epidermis, such as Langerhans cells, melanocytes or Merkel cells (Al-Barwari and Potten, 1979; Argyris, 1976). Mammalian epidermis is composed by the interfollicular epidermis with associated hair follicles, sebaceous glands and sweat glands, and there are stem cells in different locations, that maintain all epidermal lineages (Jones et al., 2007; Owens and Watt, 2003). The epidermis is in a constant state of proliveration keeping a balance between self-renewal and differentiation. An unbalance of this system could lead to diseases or cancers (Owens and Watt, 2003; Perez-Losada and Balmain, 2003) . Several stem and progenitor cell types have been identified in the skin epithelium (Blanpain and Fuchs, 2009; Jaks et al., 2010; Jensen et al., 2009). Epidermal stem cells are the most accessible of all adult stem cells and they can be easily cultured and expanded (Limat and Noser, 1986; Rheinwatd and Green, 1975; Rochat et al., 1994). Most eminent stem cells in the epidermis are hair follicle stem cells, that are known as the bulge (Cotsarelis et al., 1990). These stem cell lineages are already specified during embryonic development and are responsible for tissue homeostasis throughout life (Benitah and Frye, 2012; Jensen et al., 2009). All skin epithelial lineages express TRP63, which is a squamous epithelial fate determinant (Botchkarev and Flores, 2014; Mills et al., 1999; Truong and Khavari, 2007).

Identification of self-renewing cancer stem cell (CSCs) showed that tumors can sustain long term growth and that are hierarchically very well organized (Clarke et al., 2006). In general, these CSCs reside in so called niches that and provide them with specific microenvironment (Fuchs et al., 2004; Watt and Hogan, 2000). Epidermal and hair follicle stem cells do not interchange cell fates during homeostasis, with the exception that they can upon regeneration of tissue when wounded (Ito et al., 2005; 2007).

Squamous cell carcinomas (SCCs), the second most common type of skin cancer, are potentially deadly and belong to the most frequent cancers in humans (Alam and Ratner, 2001). SCCs become malignant when Trp53 function has been disrupted after benign papillomas ectopically activate oncogenic Ras (Brown et al., 1998; Greenhalgh et al., 1993; Lapouge et al., 2011; White et al., 2011). SCC are hierarchically very organized and are maintained by tumor propagating cells (TPCs). These TPCs can self-renew and differentiate and are located in the basal layer of the tumor (Driessens et al., 2012; Pierce and Wallace, 1971). TPCs can be isolated from the tumor based on their expression of high $\alpha 6\beta 4$ and $\beta 1$ integrin and Epcam (Lapouge et al., 2012; Schober and Fuchs, 2011). In vitro these cells also self-renew and can establish secondary SCCs if transplanted into the dermis of recipient mice, whereas $\alpha 6\beta 4$ and $\beta 1$ low cells do not have a tumor initiating potential (Schober and Fuchs, 2011).

TPCs show a unique expression pattern that differs from normal epithelial progenitors (Arnold et al., 2011; Lien et al., 2011; Siegle et al., 2014). Differential gene expression analysis showed that genes involved in normal skin epithelial stem and progenitor maintenance are not expressed in TPCs (Latil et al., 2016; Yang et al., 2015). TPCs instead de-novo express Sox2 (Schober and Fuchs, 2011; Siegle et al., 2014), and Pitx1 (Siegle et al., 2014)(Sastre-Perona et al; submitted) transcription factors. This suggests that self-renewal in normal skin and in TPCs could be controlled by different mechanisms. Sox2 is required for carcinogenesis, tumor cell proliferation, survival and clonal expansion (Boumahdi et al., 2014), but it is not required in normal skin development and homeostasis. In addition Pitx1 and Sox2 are epigenetically repressed and undetectable in normal skin (Arnold et al., 2011; Lien et al., 2011). These findings provide a powerful possible target for effective SCC therapies as it could provide a way to directly target TPCs.

Sox2 and Pitx1 are exclusively expressed in the nucleus of TPCs, but they are not expressed in differentiated SCCs, that do not have the ability to proliferate anymore. Moreover, depletion of Sox2 and Pitx1 with different approaches causes a lost of tumor formatting potential and maintenance, in addition to loss of secondary tumor formation capacity. All of these findings suggest that SCCs are ectopic grows, rather than uncontrolled tissue growth. This is especially significant as it would

provide a way of targeting these tumors without disrupting the normal skin environment (Siegle et al., 2014).

Sastre Perona et al. (submitted) show, that Pitx1 and Sox2 cooperate with Trp63, a squamous lineage defining transcription marker, forming a transcription factor network specific to SCCs that maintains TPC self-renewal. This specific networks of TPCs acts as a bi-stable switch that represses Klf4 expression in the suprabasal layer and this way blocks differentiation. Even though, this network is similar to the embryonic stem cells it is dissimilar (Young, 2011). If Pitx1 gets lost from the self-renewal circuit, Klf4 gets induce, triggering the squamous differentiation program. In addition, Pixt1 and Klf4 are inversely correlated, suggesting that Pitx1 directly represses Klf4. ChIP-sequencing analysis showed that Pitx1 represses Klf4 by binding to its downstream enhancer and knock down of Pitx1 increases Klf4 levels in TPCs. On the other hand Klf4 also represses Sox2 and Pitx1 in the suprabasal cell layer (Sastre-Perona et al.; submitted).

CRISPR-a and CRISPR-i dCas9 system

CRISPR-Cas9 is a widely used system that has proven to be a milestone discovery. It is an RNA-guided adaptive immune system that has been adapted for targeted DNA cleavage in prokaryotic and eukaryotic genomes. (Charpentier and Doudna, 2013). In the characterized type II CRISPR/Cas system, a ribonucleoprotein complex formed from a single protein (Cas9), a crRNA, and a trans-acting crRNA (tracrRNA) execute efficient crRNA - directed recognition and foreign DNA can be cleaved site-specific (Jinek et al., 2012)(Deltcheva et al., 2011). A double strand break is induced (Jinek et al., 2012).

The CRISPR-dCas9 system includes a catalytically deactivated Cas9 (dCas9) that lacks the endonuclease activity so therefore targets the genomic DNA without cleaving it (Qi et al., 2013). This method has been formerly published by (Gilbert et al., 2013; Larson et al., 2013). CRISPR-dCas9 interferes transcription elongation by blocking RNA polymerase or interferes with transcription factor binding (Larson et al., 2013; Qi et al., 2013). Adaptations of this method can provide a powerful tool to silence or activate a gene in a targeted manner. In order to potently silence a gene, the dCas9 can be fused to a repressive effector like KRAB, a repressive chromatin

modifier domain. This setup has been called the CRISPR-i system (CRISPR interference). In order to activate a gene, the dCas9 can be fused to an activating effector, like VP64, a synthetic transcriptional activator (Gilbert et al., 2013; Hsu et al., 2014; Larson et al., 2013). This method has also been called CRISPR-a (activating CRISPR). To achieve an stronger transcriptional activation or repression, using multiple sgRNAs targeting the same promotor can be beneficial (Mali et al., 2013; Perez-Pinera et al., 2013). This needs to be done in a careful way as the right position from one of the guide RNAs is also important, as for example if the two sgRNAs are too close together repression can actually be impared (Qi et al., 2013). Both CRISPR–a and CRISPR–i can be fused to a inducible TRE promoter (Kearns et al., 2014). One of the big advantages of this system is, that is has a very low number of off target effects and further is multiplexable. (Qi et al., 2013). For the activation of a gene (with the fusion of the VP64) can be enhanced with the use of multiple sgRNAs (Kearns et al., 2014). It is also possible to co–express two sgRNA that target two separate genes and knocked down both genes independently at the same time. One important factor about the sgRNAs is the distance to the transcription start site (TSS) as mentioned in (Qi et al., 2013). They showed that there is an inversely correlation between the target distance and from the TSS. Here a distance of -50 to +300 bp from the TSS proved to be optimal (Dominguez et al., 2015). Furthermore an optimal length of the sgRNA is described with 20bp, but could be cut down to a minimal base-pairing of 12 bp for sufficient gene silencing (Qi et al., 2013).

Aims

This project was part of a bigger project that led to a paper that is currently submitted (November 2018). This means that all data shown in this report are confidential. In this report I focused just on work that I had performed, not the whole paper with the work also performed by others.

The main question of this project was **how Pitx1 interacts with and represses Klf4**. Experiments by Sastre-Perona et al. (submitted) showed that Sox2, Pitx1 and Trp63 function in a positive feed-forward loop to govern self-renewal and block differentiation. Pitx1 binds to the Klf4 enhancer to repress its expression, and this way blocks differentiation of TPCs. As Klf4 is also repressing Sox2 and Pitx1 in the supra-basal cell layer the question now is how the switch from self-renewing in the basal layer to differentiation in the supra-basal cell layer happens. To answer this question I performed a variety of experiments including knock-out of Klf4 enhancers and CRISPR-a and CRISPR-i to achieve a physiological overexpression of Klf4 and a repression of Pitx1. This way I want to help solving the puzzle how the cell fate changes on TPCs from SCCs.

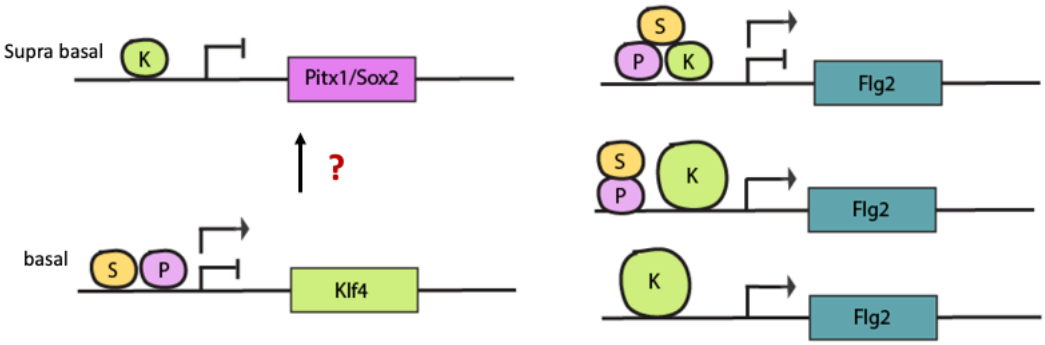

Figure 1: Schematic depiction of the aim of this project. Sox2 (yellow), Pitx1 (pink), Klf4 (green), Flg2 (blue). On the left side:t the switch of Klf4 repression by binding of Sox2 and Pitx1 in the basal layer and Klf4 binding to repress Pitx1 and Sox2 in the supra basal layer. On the right: Possible ways of Klf4 inducing differentiation include a competition with Sox2 and Pitx1 that could require higher levels of Klf4 to induce differentiation. Another possibility is that Klf4 binding alone is sufficient enough.

Material and Methods

Cell Culture

Primary murine SCC-TPC lines were generated from malignant tumors induced with DMBA following the complete carcinogenesis protocol as previously described (Guasch et al., 2007; Schober and Fuchs, 2011; Siegle et al., 2014) . Cells were split using Trypsin and maintained in E low Ca2+ (0.05mM) media.

For the generation of cell lines VSV–G pseudotyped lentivirus was made with Lipofectamine 2000 according to the manufacturers protocol (Invitrogen) by transfection of 293FT cells. These cells were transfected with pLKO shRNA vector or sgOpti (Addgene plasmid 85681) and the helper plasmids pMD2–VSVg and pPAX2 (Addgene plasmids 12259 and 12260). A DMEM media with 10% FBS and Pen/Strep solution was used for maintaining the 293FT cells. Supernatant containing the virus was collected 48h and 72h after the transfection and filtered through a 0.45 μm polyvinylidene difluoride filters. After plating cells for infection in a 6 well plate, a day after cells were plated they were incubated with a 1:3 virus to media mix containing 30μg/ml of Polybrene and spun at 1.100g for 30min at 37°C. Forty eight hours after infection cells could be selected with Puromycin (1μg/μl) (Sigma-Aldrich) if necessary or the respective selection marker of the plasmid.

CRISPR-a and CRISPR-i with dCas9

For the generation of Klf4 overexpressing cells a plasmid that was previously published in hESCs was used (Kearns et al., 2014). This plasmid consists of activating inducible TRE-dCas9-HA-VP64, which allows to follow the on-set of the dCas9 expression with the HA tag. Several sgRNAs for the Klf4 locus were tested and an sgRNA with a distance of 45 to the transcription start site (TSS) was working the best and used for all further experiments.

For a constitutive Pitx1 interference a LRGv2 (V) or pLVX-U6-FE-sfPac (P) (Aifantis lab, NYU Langone) backbone for the sgRNAs and a constitutive pHR-SFFV-KRAB-dCas9-P2A-mCherry backbone were used. For the inducible Pitx1 interference the sgOpti (O) backbone was used for the sgRNA in addition to an

inducible TRE-KRAB-dCas9-IRES-GFP (Addgene plasmid 85556). For both the constitutive and inducible Pitx1 interference 5 different sgRNA were used:

Distance to TSS	Name (dependent on backbone)
1	V1/O1
73	V2/O2
27	V3/O3
98	V4/P4/O4
120	V5/P5/O5

These guide RNAs were either used on their own or in a combination with a second sgRNA as this was shown to possibly improve the effect (Qi et al., 2013).

Klf4 enhancer deletion was performed with two *sgRNAs* flanking Pitx1 and Klf4 bound regions. sgRNA against dTomato was used as a control. sgRNA sequences were cloned into pLKO U6-puro or GFP-modified vector (Addgene 52963). After sgRNA transduction, cells subsequently infected with lentiCas9-Blast (Addgene 52962), and selected with Blasticidin for 3 days (5µg/ml). An shScr (Scramble) was used as a negative control.

Mice

6-week-old, female Nude (NU/NU [088] Charles River) mice were used for orthotopic transplantations and xenograft studies. Tumors were detected by palpation, measured with digital calipers to calculate tumor volumes (VTumor . π/6xlxw2, where l=length in mm and w=width in mm). Mice were injected with 50 mg/g EdU (Invitrogen, A10044) intraperitoneally 6hrs before sacrifice. For inducible shRNA or sgRNA expression in tumors, mice were placed on doxycycline-containing (200 mg) chow once tumors were established. Tumor volume was measured every day for 10 days. All animal experiments were performed in accordance with the guidelines and approval of the Institutional Animal Care and Use Committee at New York University Langone Medical Center.

Quantitative reverse-transcription PCR

mRNA was isolated using Qiazol (Qiagen) and Direct-zol RNA Mini Prep Kits (R2052, Zymo Research). Samples were quantified using a Nanodrop spectrophotometer (Thermo Scientific). Complementary DNA was synthesized from 1.5µg of total RNA using SuperScript VILO with random primers (Invitrogen). qRT–PCR was performed with FastStart Universal SYBR Green Master (Rox) (10802200, Roche) on a StepOnePlusTM Real-Time PCR System (Applied Biosystems). Measurements were recorded in triplicate. Differences between samples and controls were calculated based on the 2-ΔΔCT method and normalized to Rplp0.

Western blotting

Cell lysates from cultured cells were prepared using RIPA buffer (150mM sodium chloride, 0.1% Triton-X 100, 0.5% SDS and 50mM Tris pH 8 in ddH2O) with complete Mini EDTA-free protease inhibitor tablets (04693159001, Roche). Protein concentrations were determined following the instructions of Pierce BCA Protein Assay Kit (23225, Pierce). Lysates were boiled with 5x Laemmli buffer (6% SDS, 15% β- mercaptoethanol, 30% glycerol, 0.006% bromophenol blue, 0.188M Tris–HCl) for 10 min at 95°C. Protein ladder used was Full-Range Rainbow Molecular Weight Markers (RPN800, GE Healthcare). 30µg of protein was loaded per lane. Gel electrophoresis was performed using a 10 or 12% Bis-Tris gel run for 75–150min at 100V, gel was transferred for 1h – 1.5h at 4°C at 100V to a 0.45µm nitrocellulose membrane (Whatmann) and transfer was assessed by Ponceau S staining (0.1% (w/v) Ponceau S in 5% (v/v) acetic acid). Membranes were blocked with 5% non-fat dry milk in TBST, then incubated with primary antibodies diluted in blocking overnight at 4°C with gentle agitation. Membranes were rinsed with TBST before incubating with horseradish peroxidase-conjugated secondary antibodies diluted in blocking buffer for 1h at RT. Membranes were washed with TBST before incubating with Supersignal West Pico or Femto Chemiluminscent substrate (Life Technologies, #34080 add #30095) and exposed to X-ray film (F-9024-8_10, GeneMate) using a Kodak X-Omat 2000A Processor. Antibodies used for western blotting were SOX2 (1:1,000; Abcam, ab92494), KLF4 (1:1,000; R&D, AF3758), TP63 (1:1,000; Cell Signaling, 13109), PITX1, (1:500; Santa Cruz, 18922), Tubulin (1:10,000; Sigma,

T5201), Vinculin (1:10000; Sigma, V9131), CASPASE-3 (1:1000; Cell Signaling, 9664S), Filaggrin (1:1000; BioLegend, 905801).

Immunofluorescence and imaging

Unfixed tumors were embedded in OCT (Tissue Tek) and after freezing cryo sectioned into sections of 10μm on a Leica cryostat and mounted in SuperFrost slides (Fisher). For staining the slides were airdried for 10min after taking them out of -80°C and fixed with 4% Formaldehyde for 10min. Then slides were rinsed and permeabilized with 0.5% Triton X-100 in PBS for 15min followed by blocking in PBS with 5% donkey serum, 1%BSA and 0.3% Triton X-100. The primary antibody was incubated overnight at 4°C. After washing with PBS, secondary antibodies, conjugated to Alexa 488, Alexa FITC, Alexa 568, DyLight 649, and Hoechst 33342 (83218, AnaSpec) were diluted in blocking buffer and incubated on the slides for 1hr at room temperature. After washing, slides were mounted in ProLong Gold (Invitrogen). Imaging was performed on a Nikon Eclipse TiE Microscope or a Zeiss LSM780 Confocal Microscope. Images have been analyzed in NIS-Elements, Zen software or ImageJ. Antibodies for immunofluorescence were CD49f (1:200; Biolegend, 313618), SOX2 (1:1000; Abcam, Ab92494), PITX1 (1:500; Novus, NBP1-88644), and Filaggrin (1:1000; BioLegend, 905801) (according to Sastre-Perona et al., submitted).

Primer sequences

	sgRNA oligos KLF4 Enhancer
gRNA Klf4_Pk1_1	ACTTGGCCACACTGCGGTTG
gRNA Klf4_Pk1_2	GGTCACAACCAAAATGCGGC
gRNA Klf4_Pk2_1	GGTGCGGAGCATGAGATCAC
gRNA Klf4_Pk2_2	GTTTGAAATGACTTACCTTGT
	sgRNA oligos CRISPRi
gRNA CAG	GTTCCGCGTTACATAACTTACGG
gRNA Pitx1_1	AGGGAGAGAGGGAGGGAGGG
gRNA Pitx1_2	AGGGGGGGAGGTGAGGCGGC
gRNA Pitx1_3	GCGGGCGAGGCCAGGAGGGA

QPCR oligos	
Sox2_Forward	GGGGCAGCGGCGTAAGA
Sox2_Reverse	AGCCTCCGGGAAGCGTGTA
Pitx1_Forward	CCGGGATGCCAGGAAGAGC
Pitx1_Reverse	CACGGGCAGGCGGACAGT
DNTrp63_Forward	CCTGGAAAACAATGCCCAGACT
DNTrp63_Reverse	AGGAGCCCCAGGTTCGT
Klf4_Forward	GACTAACCGTTGGCGTGAGG
Klf4_Reverse	GTCTAGGTCCAGGAGGTCGT
Krt1_Forward	GACACCACAACCCGGACCCAAAACTTAG
Krt1_Reverse	ATACTGGGCCTTGACTTCCGAGATGATG
Krt10_Forward	GGAGGGTAAAATCAAGGAGTGGTA
Krt10_Reverse	TCAATCTGCAGCAGCACGTT
Flg2_Forward	GGAGGCATGGTGGAACTGA
Flg2_Reverse	TGTTTATCTTTTCCCTCACTTCTACATC
Rplp0_Forward	GTGCCATCGCCCCGTGTG
Rplp0_Reverse	TGGATGATCAGCCCGAAGGAGA

Results

Inducible overexpression of Klf4

The Dox-inducible CRISPR-a dCas9 system was used for physiological KLF4 overexpression. After testing 4 different sgRNAs targeting different positions of the klf4 TSS, the sgRNA 1 (called K-1) showed the most promising results (data not shown) and was used for further experiments. The K-1 sgRNA was 45 bases away from the TSS and was the one most proximal that was tested. The K-1 sgRNA is always compared to a control sgRNA (CAG) that targets an artificial promoter (CAG promoter).

To compare our dCas9 activation (Shown as HA) to previous published data (Kearns et al., 2014), we performed a time course with 3 different SCC cell lines that have been infected with an inducible TRE-dCas9-HA-VP64. In this time course cells were put on Doxycycline (Dox) for up to 6 days.

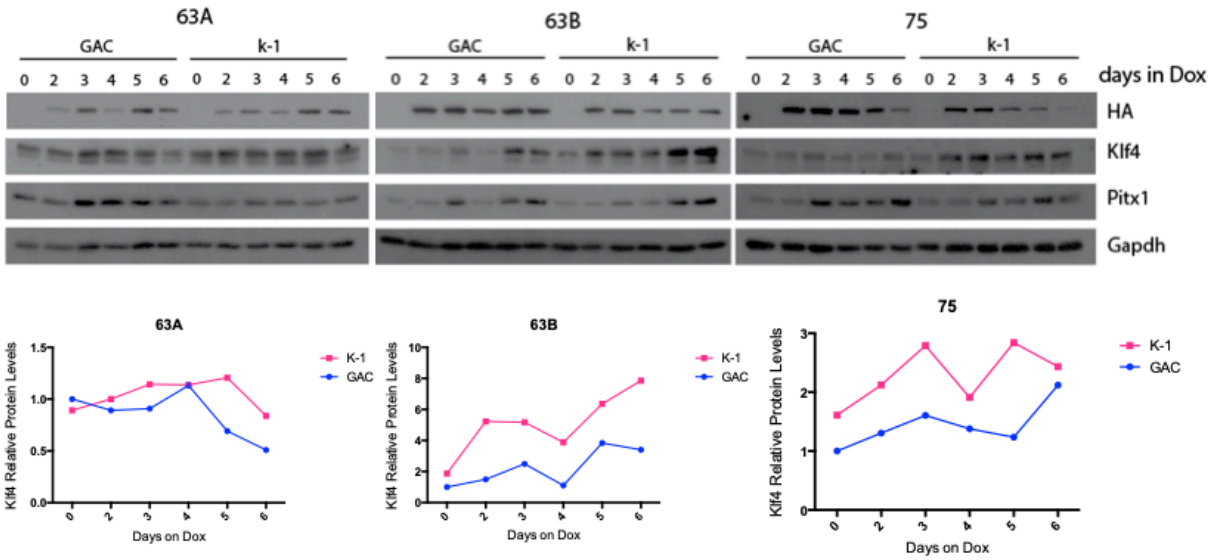

Figure 2:Three different primary murine SCC-TPC cell lines, namely 63A, 63B and 75, that express a TRE-dCas9-HA-VP64 and a sgRNA for Klf4 45 bases upstream from the TSS. Upper row shows the Western blots of the 3 cell lines with the control (CAG, blue) on the respective left side of the blot and the Klf4 over expressing cells (K-1, pink) on the right side. Stainings were performed for HA, Klf4 and Pitx1. Vin was used as a loading control. A timecourse for the expression of HA was achieved in putting the cells on Dox for 0 up to 6 days. Expression of HA can be seen in all three different cell lines. The bottom 3 graphs show a quantitative analysis of the same western blots shown in the first row. Again there is a timecourse, describing how long cells have been on Dox. Relative protein levels of Klf4 fluctuate, but an overall trend of an increase can be seen in SCC 63B and 75. Analysis was done in FIJI and normalized to 0 days on Dox..

We could detect HA expression, and therefore the dCas9, in all 3 cell lines after Dox addition. In comparison to (Kearns et al., 2014), we see expression already after 2 days on Dox. Unfortunately, just in two out of three cell lines the right trend of Klf4 overexpression could be observed. The slight increase of Pitx1 can be due to the reason, that wells were confluent by Day 6.

To additionally test if Klf4 expression can be further increased, cells were switch into High Ca^{2+} media (1.5 mM). This can push cells to differentiate, as described in Sastre-Perona et al., submitted and previously in … . These condition is in comparison to Low Ca^{2+} , in which cells are still proliferative and undifferentiated. To test if this enhances Klf4 levels, we use several TRE-dCas9-HA-VP64 cell lines, incubate them on Dox for two days, and then switch them to high Ca^{2+} media for 0h, 16h or 24h. At the end of the experiment, we extracted protein and performed western blots analysis on different TRE-dCas9-HA-VP64 cell lines and put cells on Dox for two days. After these two days cells were put in high Ca^{2+} for 0h, 16h or 24h.

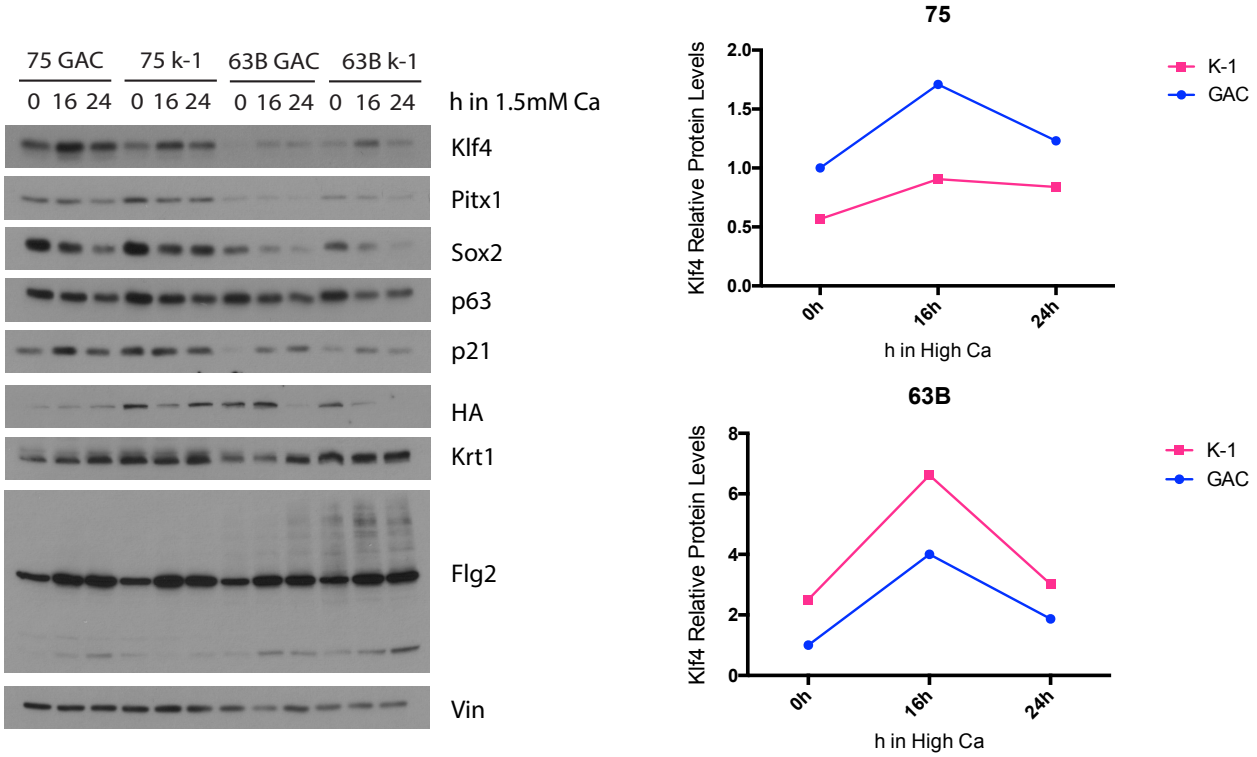

Figure 3 The left part of the graph shows western blots performed on 2 cell lines which have been put on Dox for 2 days followed by 0 up to 24h on high Ca^{2+} media. An increase of Klf4 can be seen in addition to an increase of the differentiation maker Flg2 and Krt1.On the right side a quantitative analysis of the western blot show the relative protein levels of Klf4. Vinculin is used as a loading control.

As previously seen in the lab, there is already an increase in Klf4 in CAG control cells, when the cells are put in High Ca^{2+} differentiation media. And this increase is further increase in the K-1 sgRNA cells. The increase in Klf4 also results in a higher induction of Flg2 and Krt1 expression, reflecting a more differentiated phenotype. The best increase of Klf4 expression can be achieved with 16h in High Ca^{2+} media. 24h of High Ca^{2+} media might be too long as it might push cells already too far in the differentiation program, suggested by the further increase in Flg2 and Krt1 and a loss of Klf4 in the controls CAG. These cells would then rather mimic the differentiated and enucleated cells that go on to form keratin pearls. On the other hand, these results could be just obtained in the 63B SCC line, so this cell line was used for further characterization of this physiological overexpression of Klf4.

With these outcome we went further and performed RTqPCR on 63B SCCs to characterize these cells also on an RNA level. Our RTqPCR data confirmed the increase in Klf4 levels that we already observed in the western blot. In accordance with the western blots the highest levels of Klf4 expression can be seen after 16h in High Ca^{2+} media. In RTqPCR analysis it can also be observed that Pitx1 levels are reduced when comparing the time course of CAG control with cells infected with the sgRNA K-1.

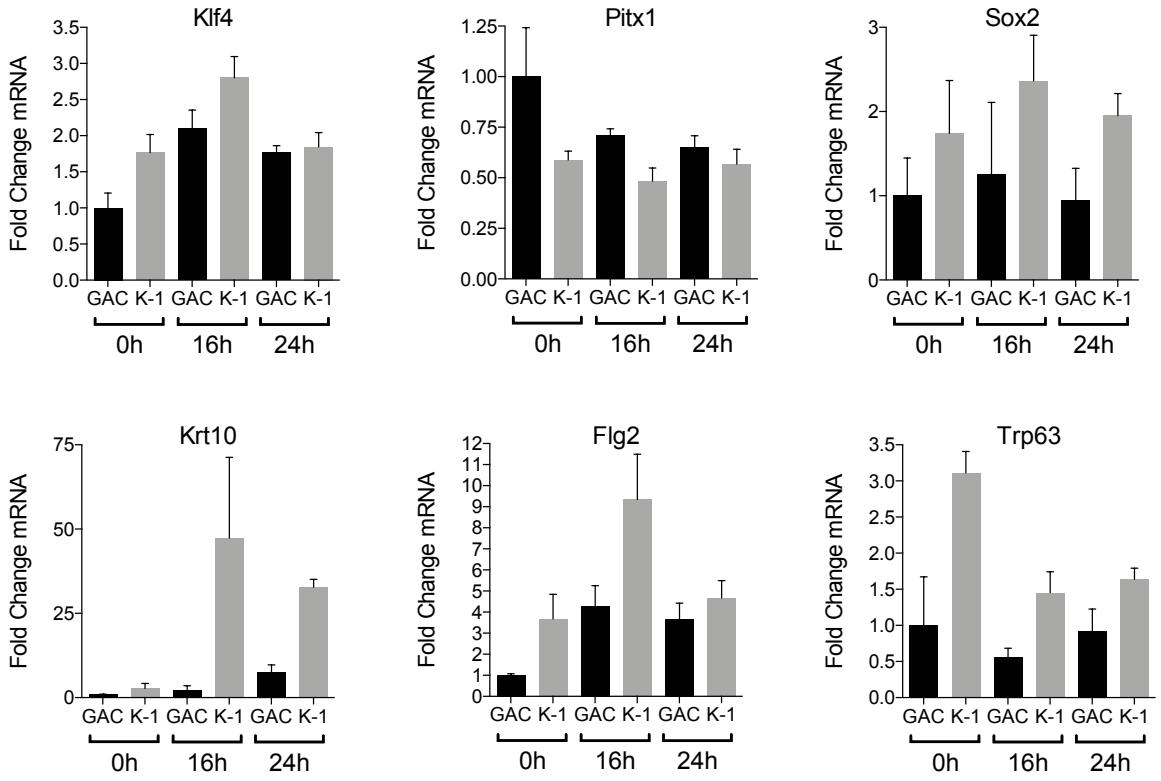

Figure 4: RTqPCR results of Klf4 overexpressing TRE-dCas9-HA-VP64 63A SCC cell line. mRNA fold change can be seen for the pluripotency regulating network (Pitx1, Trp63 and Sox2), the differentiation marker of the supra basal cells Klf4 and the differentiated cell markers Flg2 and Krt10. Cells are put on Dox for 2 days, followed by High Ca^{2+} media for 0h, 16h or up to 24h. Klf4, Krt10 and Flg2 are the highest in the K-1 cell line after 16h of High Ca^{2+} . Levels of Klf4 are going down again after High Ca^{2+} media for more than 16h (as seen in 24h). CAG SCC cell lines were used as a control cell line and results are normalized to CAG and the respective timepoint.

mRNA fold change of Sox2 and Trp63 were not further investigated in this experiment, as this with another ongoing project in the lab.

To see if this physiological overexpression of Klf4 results in changes in growth in vitro, growth curve experiments were performed for 6 days. In contrast to our expectations, the cell lines did not show any change of the growth rates in-vitro.

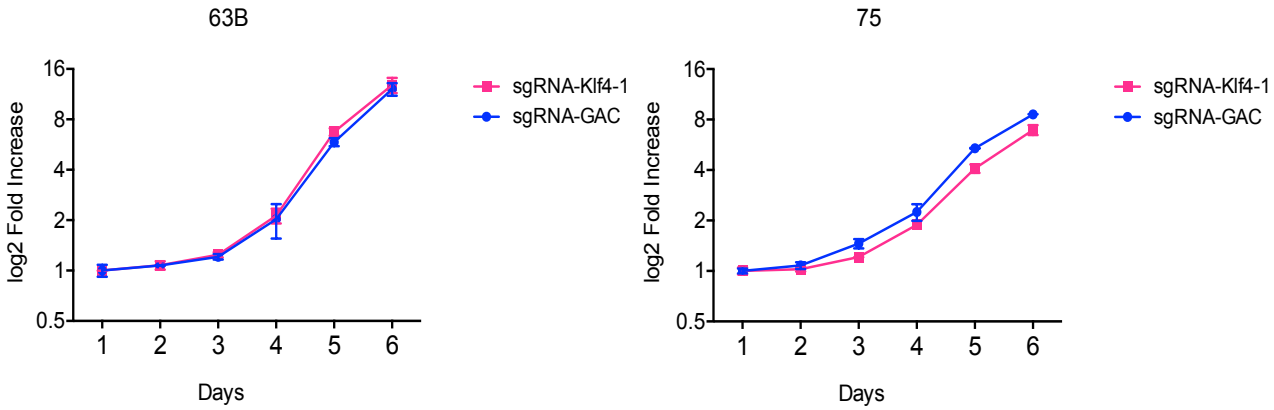

Figure 6: log2 Fold Increase of growth curves, normalized to the starting concentration at Day 0. The same can be observed in SCC 63A and 75. There is no difference between the control cells infected with the GAC sgRNA and the Klf4 overexpressing K-1 infected cell lines. Values are normalized to the starting concentration. 5000 cells were seeded into a 24 well plate.

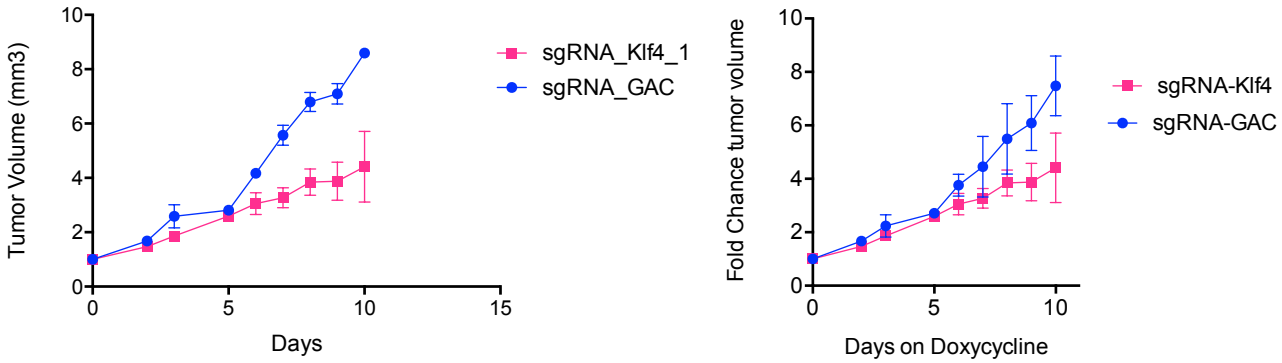

Figure 5: In contrast to in-vitro data, this graph shows that tumor growth is affected in 63B SCC cell lines in-vivo after mice are put on Dox for up to 10 days. In the SCC 63B cell line with the control sgRNA CAG shows a reduced growth compared to the K-1 sgRNA.

To investigate if Klf4 overexpression affected tumor growth in-vivo, these cells were injected into mice (this experiments were performed by Ana Sastre-Perona, as I was not allowed to handle mice myself).

After the cells were injected, we let the tumors growth until they reach 100mm^3 and them feed the mice with food containing Doxycycline (200mg/Kg) and measure the tumor volume over 10 days. This experiments show that Klf4 over-expression can reduce tumor growth.

With these results we conclude that the CRISPR-a dCas9 system is working in SSC-TPC cell lines and can provide a physiological overexpression of Klf4. Klf4 upregulation results in induction of differentiation in culture and affected tumor growth in vivo after Dox induction. Future experiments should characterize the effect on tumors further, to see if these tumors are indeed less proliferative. Further the chromatin binding of Pitx1 and Sox2 could be addressed after the overexpression of Klf4.

Deletion of Klf4 Enhancers

Sastre-Perona et al show that Pitx1 expression inversely correlate with Klf4 in mouse primary SCCs. Also, Pitx1 silencing leads to an increase in Klf4 expression. These data will suggest that Pitx1 directly represses Klf4 expression. Using ChIP-sequencing we had identified a potential downstream enhancer element, bound by Pitx1, Sox2 and Trp63, and Klf4 itself. Two peaks compose this enhancer. Peak 1 (Pk-1) is predominantly bound by PITX1 and TRP63, whereas Peak 2 (Pk-2) is highly enriched for SOX2, TRP63 and KLF4. My aim was to validate if this enhancer element regulates Klf4 expression (Figure 7).

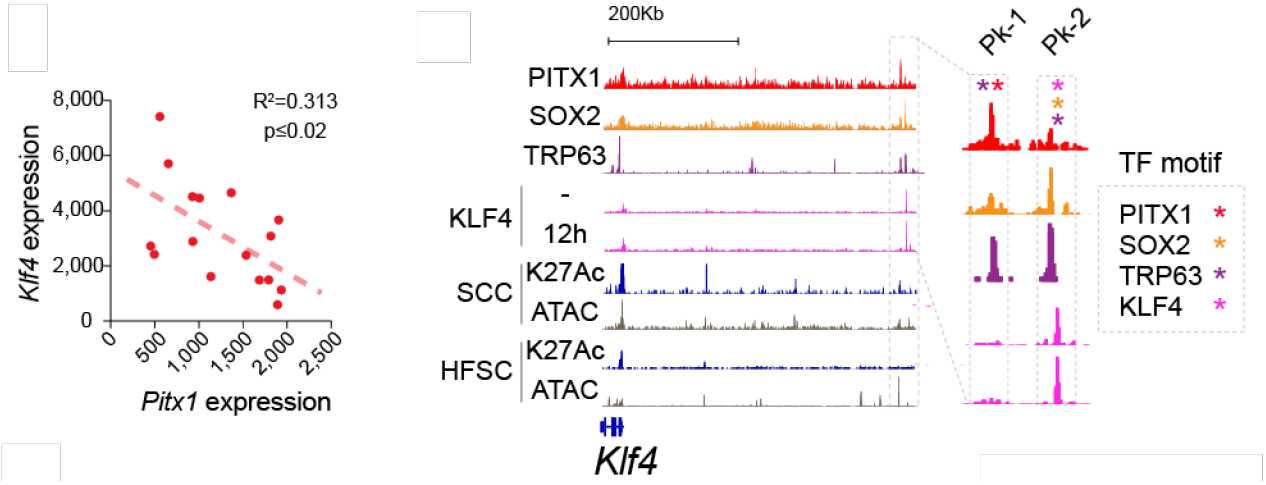

Figure 7: On the left side a Scatter plot illustrating inversely correlated Pitx1 and Klf4 expression in mouse TPCs is shown. On the right hand side ChIP-Seq tracks are displayed. PITX1 (red), SOX2 (orange), TRP63 (purple) and KLF4 (pink) at the Klf4 locus. ATAC-seq (grey) and H3K27Ac ChIP-

seq (dark blue) indicate active and open chromatin in TPCs and HFSC. Box highlights a putative Klf4 enhancer bound by PITX1, SOX2 and KLF4. Asterisks indicate TF motifs. Peak-1 and Peak-2 are shown.

In order to test this, I use CRISPR-Cas9 to delete, Enhancer 1 (Pk-1) or Enhancer 2 (Pk-2) or both Enhancers at the same time (Pk-1/2) (Figure 8).

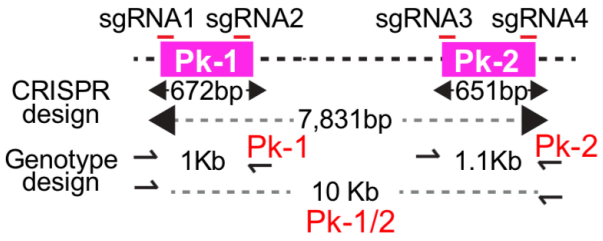

Figure 8: Schematic overview of the strategy for the deletion of the Klf4 Enhancers 1 and/or 2. This was achieved with two gRNA pairs. It can be seen that the deletion of single enhancer spanned about 1Kb, whereas the deletion of the total Enhancer (Pk-1/2) spans 10Kb.

I infected three different SCC cells with the different sgRNA combinations (Figure 8), carrying a puromycin and GFP selection marker. Then I infected the cells with a Cas9 construct, and selected the cells with blasticidin. Genotyping of the cell lines showed successful deletion of Pk-1, Pk-2 and Pk-1/2 in three different primary SCC-TPC cell lines, namely 63A, 63B and 75 (Figure 9 and 10).

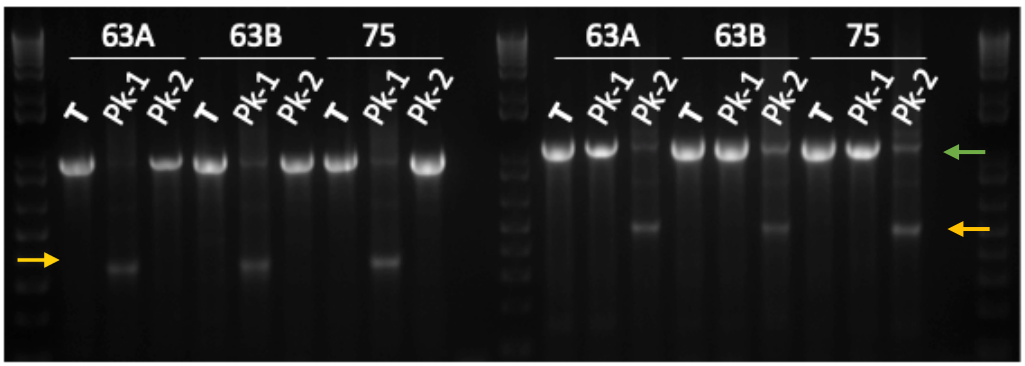

Figure 9: Genotyping of the deleted Enhancer peaks. Either Peak 1 (Pk-1) or Peak 2 (Pk-2) were deleted. The results show that there is a successful deletion of both of the peaks in all 3 different tested SCC cell lines. Tomato (T) was used as a control and shows no deletion. Green arrows indicate the WT and yellow arrows show the KO of the enhancer peak

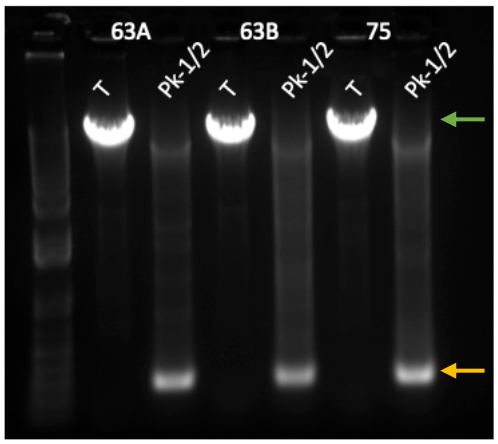

Figure 10: Genotyping of the deleted enhancer peaks. Both Peak 1 or Peak 2, called Pk-1/2, were deleted. The results show that there is a successful deletion of both of the peaks in all 3 different tested SCC cell lines. Tomato (T) was used as a control and shows no deletion. Green arrows indicate the WT and yellow arrows show the KO of the enhancer peak Pk-1/2.

Examined mRNA expression levels, the KO of the enhancer peaks shows that Klf4 expression is enhanced in SCC 63A and 75 upon deletion of Pk-1, but the same trend could not be observed in 63B SCC cells (Figure 11).

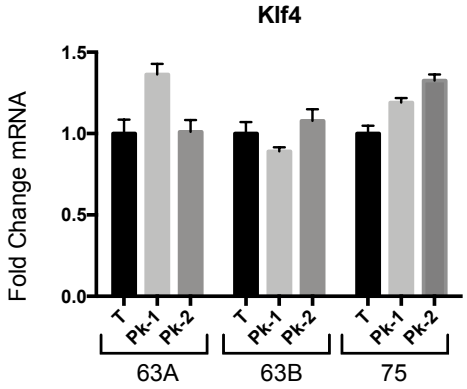

Figure 11: Klf4 expression levels detected with RTqPCR in three different cell SCC cell lines. All three cell lines are compared to a control (tomato). Fold change levels of Klf4 mRNA is shown upon Pk-1 deletion and Pk-2 deletion. An upregulation of Klf4 can be seen in the SCC 63A in Pk-1 deletion, but not in SCC 63B or 75. Values were normalized to the Tomato control.

Western blot analysis of Peak-1/2 deletion suggested the same trend in 63A. With this we decided to choose SCC 63A for further experiments.

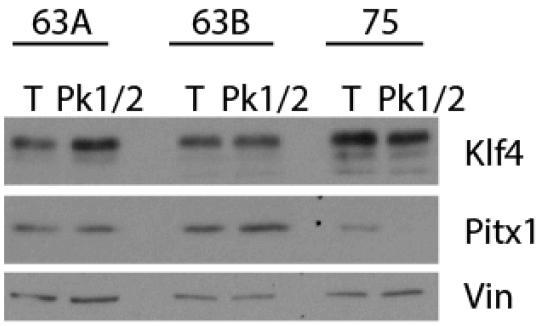

Figure 12: This figure shows western plots performed on SCC 63A, 63B and 75. Immunoblots were performed for Klf4 and Pitx1. Vinculin (Vin) was used as a loading control. An increase in the expression in Klf4 can be seen in SCC 63A, upon deletion of Peak-1/2. No such increase in the expression can be observed in SCC 63B and 75.

Since Pitx1 silencing leads to an increase on Klf4 expression, we decided to test which of the peaks in required for this effect. So, I performed a Pitx1 knock down (KD) using shRNAs on the Klf4 enhancer deleted cell lines. RTqPCR was performed on the 63A SCC line, as these showed the most promising trend in previous experiments. Pitx1 KD induced a two-fold induction in Klf4 expression compare with control shScr cells (Figure 12). This increase was further boosted on the Klf4 Pk1 and Pk2 enhancer deleted SCC cell lines, but completely abrogated on the Pk1/2 enhancer deleted cell lines. Same results were observed on the Klf4 target genes Krt10 and Flg2. RT-PCR for Pitx1 validate the efficiency of the knock-down.

All together this results indicate that: Pk1, that is bound by Pitx1, acts as a repressive element, and its deletion leads to an increase of Klf4 expression; that Klf4 or other transcription factors can further induce Klf4 expression upon Pitx1 silencing binging to either Pk1 or Pk2; that Pk1 and Pk2 are required for Klf4 induction upon Pitx1 lost.

In summary, a model where competitive PITX1 and KLF4 interaction with this enhancer element dictates Klf4 transcription in TPCs is supported as deletion of the whole enhancer Pk-1/2 provides Klf4 transcription insensitive to PITX1 and KLF4 regulation.

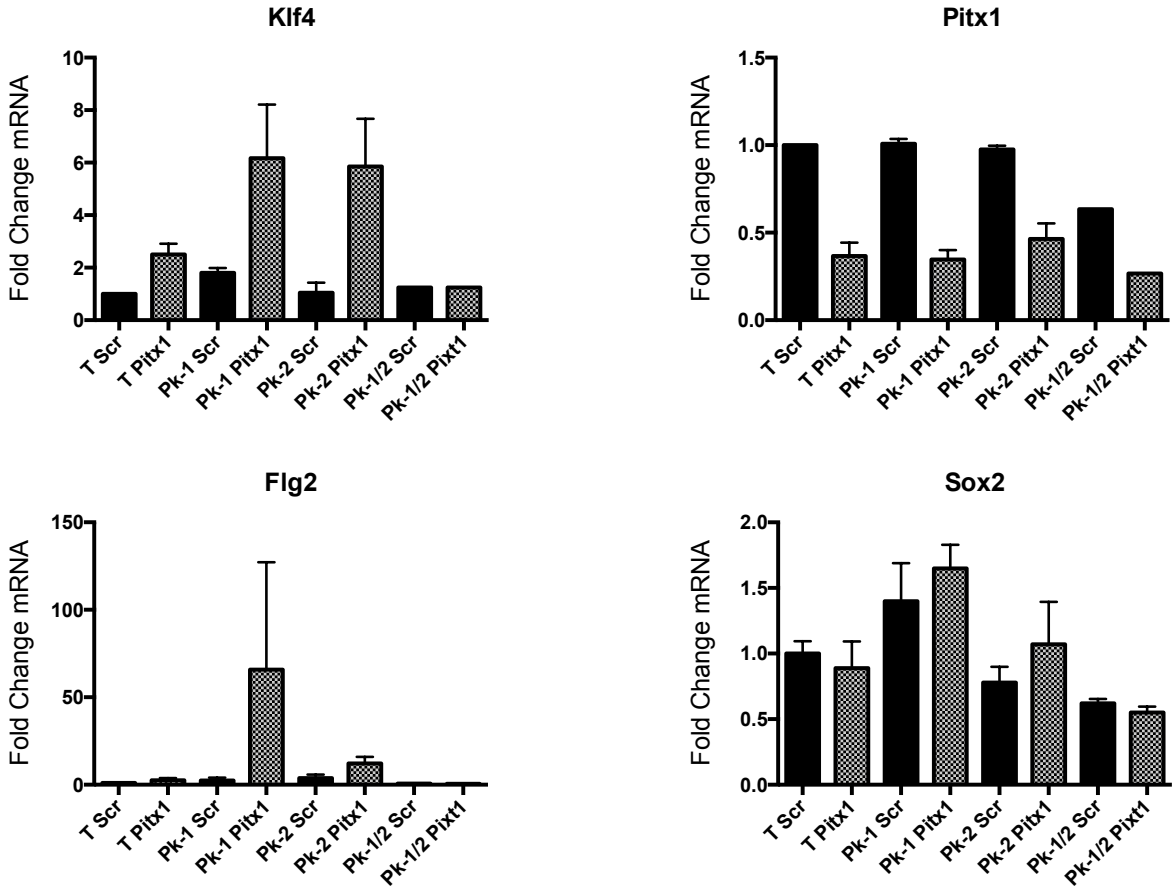

Figure 13: Fold change of mRNA Expression levels measured with RTqPCR. Here Pitx1 was knocked down in SCC cell lines that have a deletion in the Kl4 enhancer. This enhancer deletion was either in Pk-1, Pk-2 or spanning both peaks (Pk-1/2). Increased basal Kl4 expression upon Pk-1 depletion can be further increased in a Pitx1 KD. Klf4 levels upon Pitx1 loss in Pk-2 deletion increase compared to no change in expression levels without the Pitx1 KD,, as seen in the Pk-2 deletion. An increase in Flg2 levels can also be observed in Pk-1 deleted Pitx1 KD and a milder increase in SCC cell lines with a Pk-2 deletion. Scr is always used as a negative control and results ate normalized to Tomato and Scr.

Depletion of Pitx1 with an inducible CRISPR-i approach

The next aim of my project was to generate an inducible Pitx1 interference system. Pitx1 silence SCC cell lines don't form tumors and are not viable (Sastre-Perona, submitted). To evaluate the effects of a Pitx1 silencing on a pre-existing SCC tumor, I implemented a CRISPR-i approach.

First, I designed and cloned different sgRNAs binding to Pitx1 transcriptional start site (TSS) to test which distance to the TSS works the best in our system. I tested several guides, ranging from 4 to 120 bases upstream of the Pitx1 TSS using a constitutive promoter (Figure 14). For this a pHR-SFFV-KRAB-dCas9-P2A-

mCherry construct was used (Addgene 60954). sgRNAs sequences are described in the Material and Methods section.

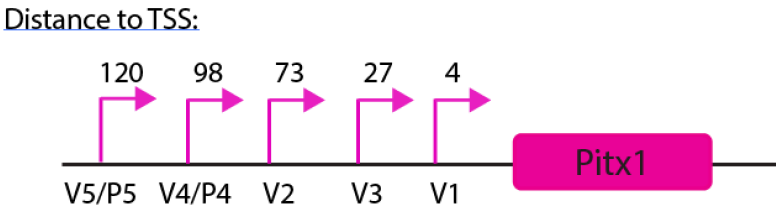

Figure 14: Graphic overview of the sgRNAs tested for inducible Pitx1 KD. Distances range from 4 to 120 bp upstream of the Pitx1 TSS. Five different sgRNAs were tested.

Results showed, that a physiological Pitx1 silencing and an upregulation of Klf4 and Flg2, can be achieved using a constitutive CRISPR-i system. RTqPCR results demonstrate that there is a wide variety of efficiency of the sgRNAs. This most likely results from the different distance of the sgRNA to the TSS of Pitx1, as this was already previously described (Qi et al., 2013).

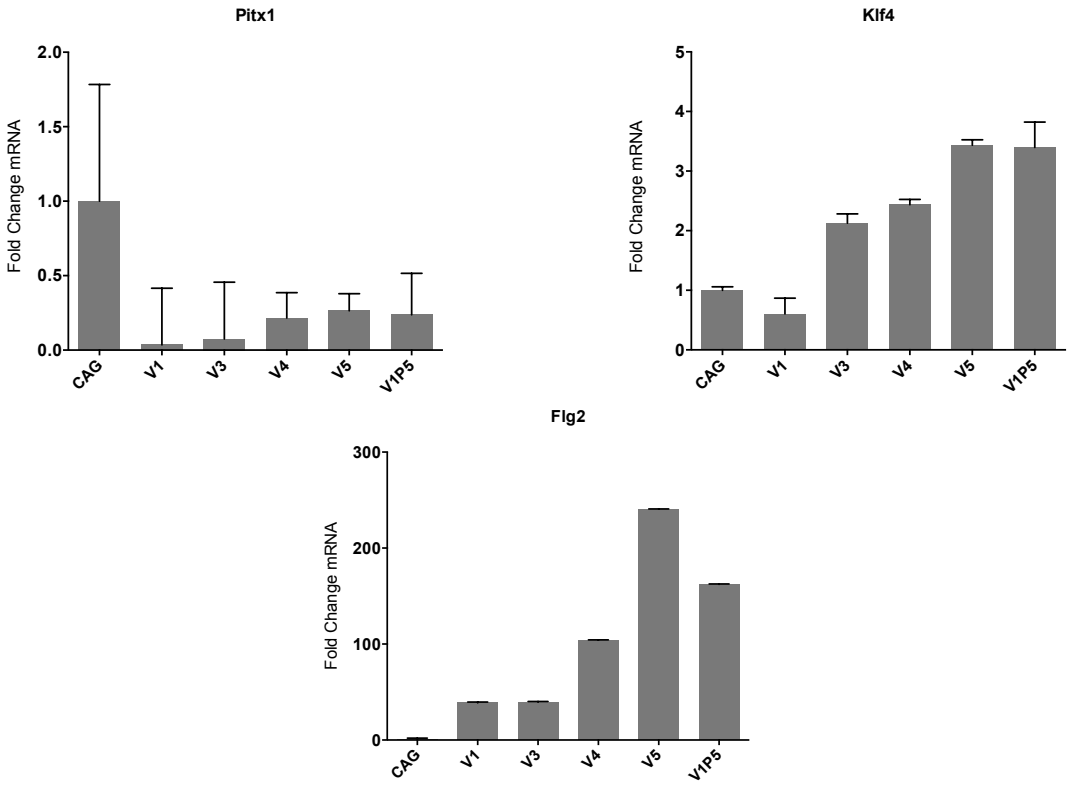

Figure 15: mRNA fold changes as seen with RTqPCR. An overall inhibition of Pitx1 can be seen, whereas an upregulation of Klf4 can just be seen in sgRNA V1 to V1P5. This shows that there is a variety in the effect that sgRNA can have. Also the use of two sgRNAs did not improve the inhibition of Pitx1. V1 to V5 are cell lines with one sgRNA, V1P5 is a cell line which has the V1+P5 sgRNA. CAG was used as a contro and results were always normalized to CAG. This experiment was performed in 63B SCC-TPCs.

To further examine how expression levels are effected on a protein level and if our cell lines express the dCas9, tagged with the HA, I performed western blots on 63B SCC cell lines that were transduced with the pHR-SFFV-KRAB-dCas9-P2A-mCherry and the different sgRNAs. These western blots showed results in accordance to the RTqPCR results (Figure 16), even though the effect was weaker and also not the same sgRNAs showed the best inhibition of Pitx1 and a further upregulation of Klf4.

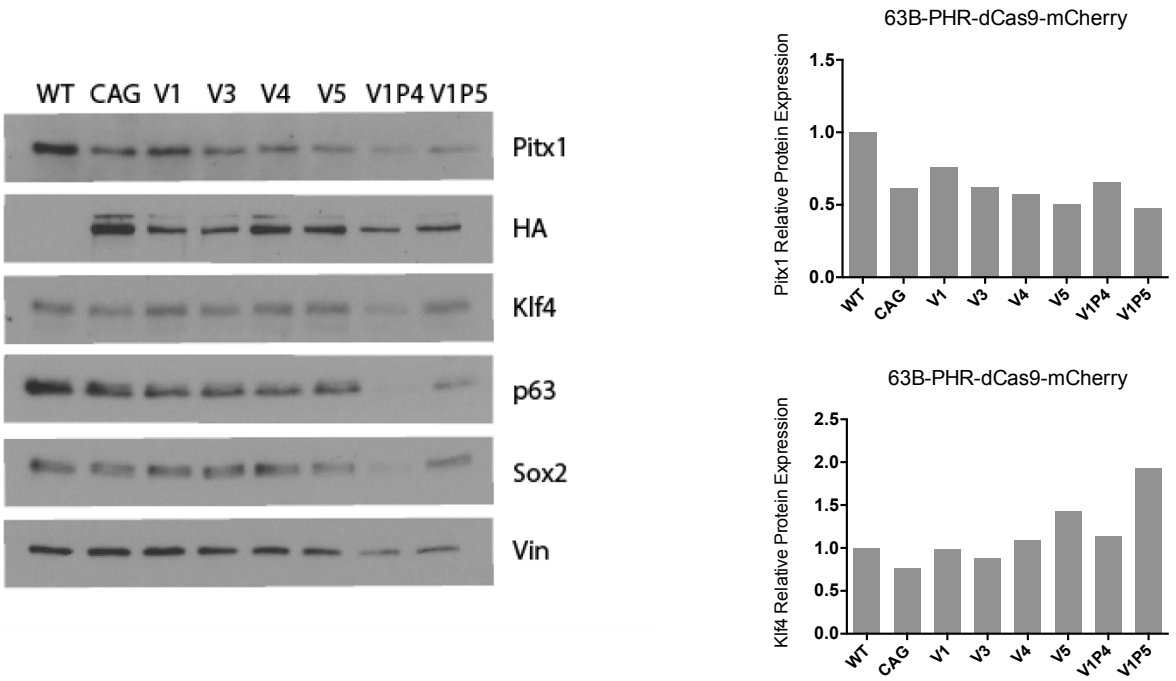

Figure 16: On the left side western blots performed on 63B SCC lines can be seen. Vinculin was used as a loading control. These western blots show an expression of HA and therefore of the dCas9. In general, there are several sgRNAs and also the combination of sgRNA V1 and P5 that show a inhibition of Pitx1 and increase of Klf4. Wild type cells (WT) were also included as a control in addition to the CAG control. Relative Protein Expression was calculated with FIJI.

Next, growth curves were performed to test if Pitx1 diminished expression correlates with an effect in growth in-vitro. No change in the growth in-vitro could be seen, except in the combination of sgRNA V1 and P5 (Figure 17).

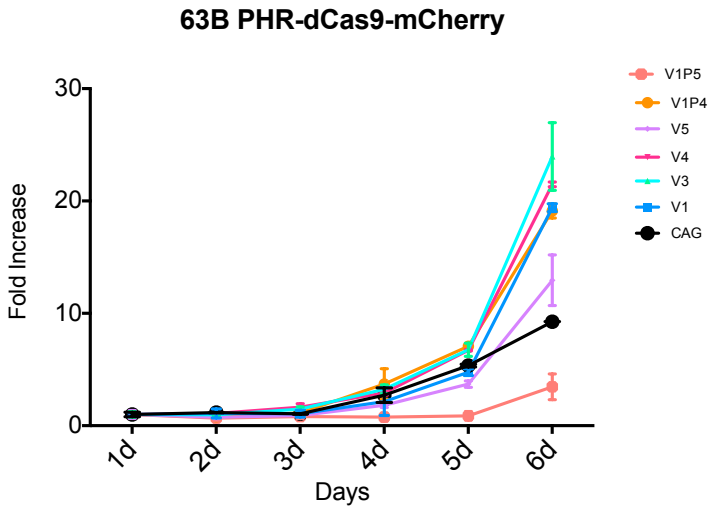

Figure 17: Growth curve of constitutive Pitx1 inhibited SCC cell lines. CAG was used as a control and is seen in black, sgRNAs V1 to V1P5 can be seen in color. There is no deficiency in growth when the control is compared to the Pitx1 inhibited SCC cell lines. The growth curves were performed over a course of 6 days with a seeding density of 5000 cells per 24well. Throughout the time course cells were kept on Dox.

As this test of the constitutive expressed pHR-SFFV-KRAB-dCas9-P2A-mCherry construct was purposed to give an idea about the distance of sgRNA most favorable in our SCC-TPC cell lines, no further optimizations were performed. Also, since the effects on Pixt1 protein levels were mild, there was no difference seen in cell growth.

Then, to answer the question of how Pitx1 silencing affects SCC growth on established SCC tumors I move to an inducible CRISPR-i dCas9 system. For this SCC-TPC cell lines were infected with a TRE-KRAB-dCas9-IRES-GFP construct (Addgene 85556). After GFP cells were selected, I infected them with different sgRNA binding at different distances to the TSS (Figure 18), to test the efficiency interfering with Pitx1 expression. Furthermore a combination of two or all three sgRNAs was also tested. All these sgRNAs were clones on the sgOpti backbone, as it contains an optimized scaffold sgRNA that help to achieve a higher efficiency of interference according to the manufacturer (Addgene).

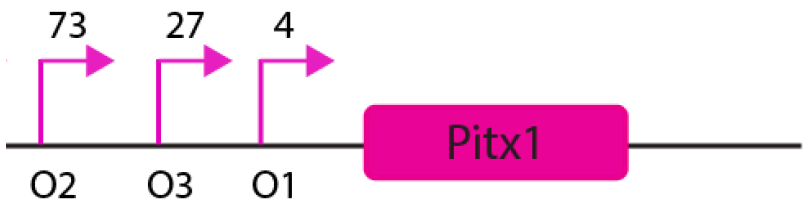

Figure 18: Schematic overview of sgRNAs used for the inducible Pitx1 interference. Three sgRNAs, O1,O2 and O3 were used. All three of them are located at a different distance to the TSS of Pitx1. Distances are indicated with the numbers above the respective sgRNA.

I induced the cells for 2 days with Doxycycline, as we have seen in previous experiments that it is sufficient, and then performed western blot. As expected, after two days a nice induction of HA-dCas9, can be seen. Importantly an inhibition of Pitx1 with several sgRNAs can also be detected (Figure 19).

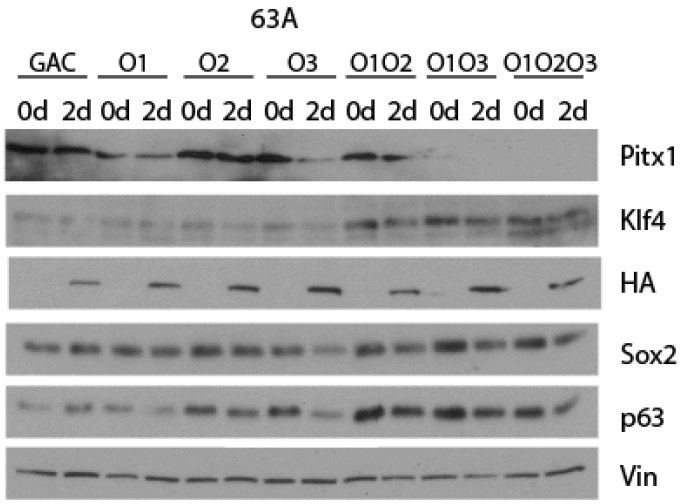

Figure 19: Western blot performed on 63A SCC-TPC. HA induction can be seen 0d versus 2d on Dox. Pitx1 expression shows a inhibited trend in several sgRNAs. Yet there is still a great variety in the expression of Pitx1 between the different sgRNAs. In addition, a decrease of Sox2 and Trp63 can be observed and correlate with the decrease in Pitx1. Vin was used as a loading control.

To see whether this trend is reproducible on an mRNA level, I performed RTqPCR. Indeed, there is the right trend of Pitx1 inhibition with several of the sgRNAs (Figure 20). Nonetheless, one of the sgRNAs, namely O3, showed the overall best inhibition of Pitx1. Taken together the results from the western blot and the RTqPCR, this O3 sgRNA was the sgRNA that was used for further experiments. O3 has an upstream distance to the TSS of Pitx1 of 27bp. In addition, the western blots showed that decreased levels of Pitx1 correlate with a decrease of Sox2 and Trp63 (Figure 19, and RTqPCR) not shown, as it was seen before using shRNAs targeting Pitx1.

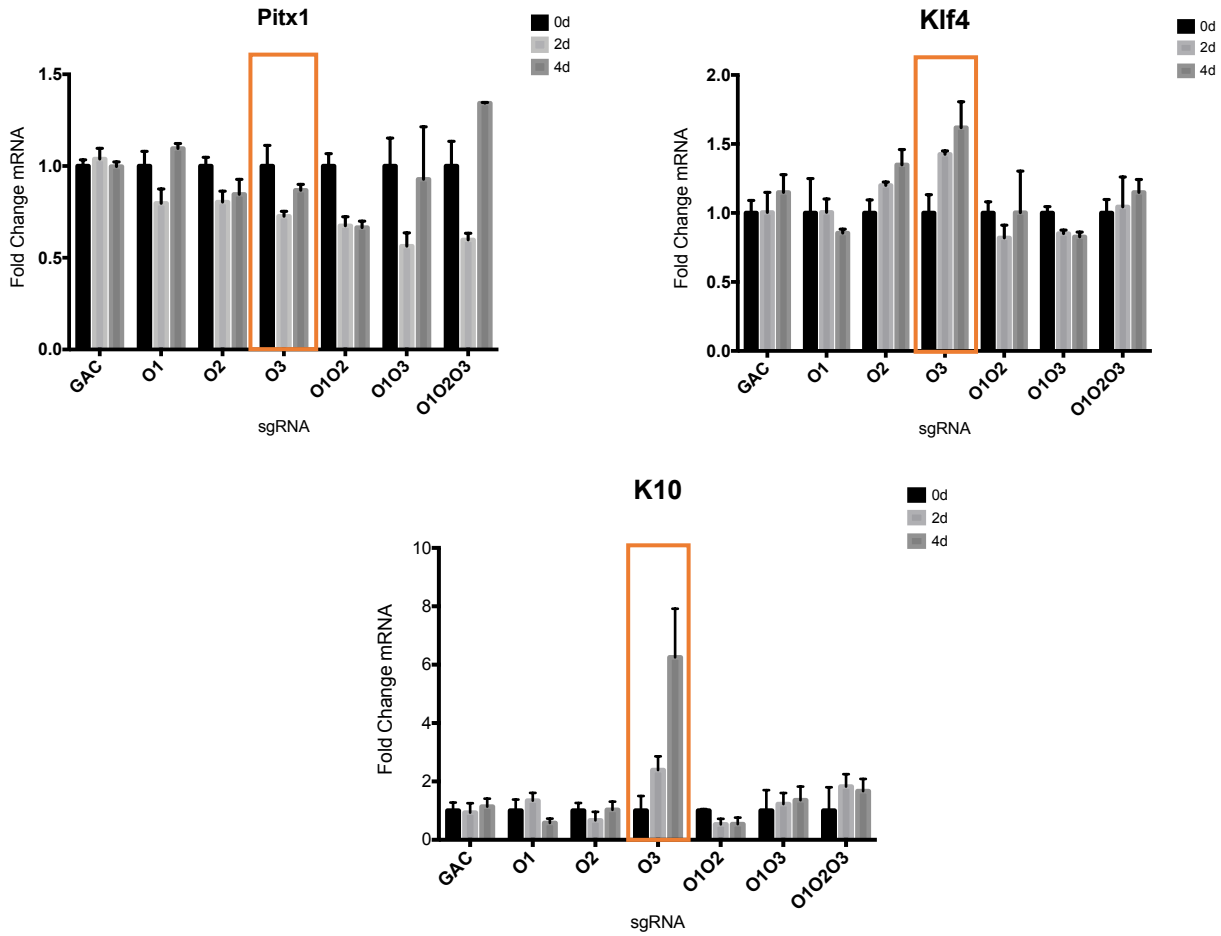

Figure 20: RTqPCR results of different inducible constructs with different sgRNA show different effects on Pitx1 expression. Also there is an increase in the expression of Klf4 and further more in the differentiation marker K10. The results of these marker show that the most promising sgRNA for the inducible TRE-KRAB-dCas9-IRES-GFP CRISPR-i construct. Cells were kept on Dox for 0d, 2d or 4d. CAG was used as a control and values were normalized to the control.

Following, we examined if Pitx1 interfering could affect the growth the cells in vitro. Indeed, growth curve experiments showed a reduced growth in Pitx1 interfered SCC cell lines, when compared to the CAG control cells (Figure 21). This was in contrast to the constitutive construct that was used to determine the distance that would suit our SCC cell lines the best. Furthermore, in the inducible system, all sgRNAs that were used showed a reduced growth. Nonetheless, the effects on growth still varied between the different sgRNA that were used.

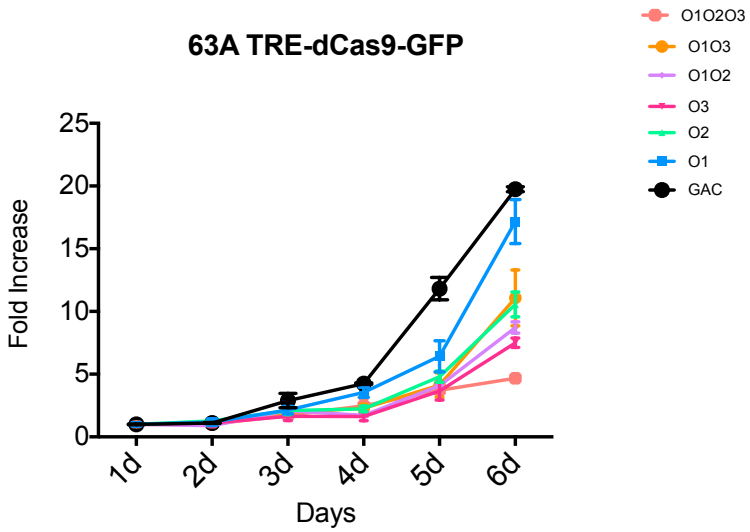

Figure 21: Growth curve of inducible TRE-KRAB-dCas9-IRES-GFP Pitx1 inhibited SCC cell lines. CAG was used as a control and is seen in black, sgRNAs O1 to O1O2O3 can be seen in color. There is a deficiency in growth the induced Pitx1 inhibited cell lines when compared with the control CAG. The growth curves were performed over a course of 6 days with a seeding density of 5000 cells per 24well. Throughout the time course cells were kept on Dox.

As in vitro experiments showed very promising results, the next step was to see the effects of these inducible Pitx1 interference in vivo. After tumors were established, mice were put on Dox to induce the TRE-KRAB-dCas9-IRES-GFP Indeed, in fact also differences in vivo could be seen by different expression levels of these markers.

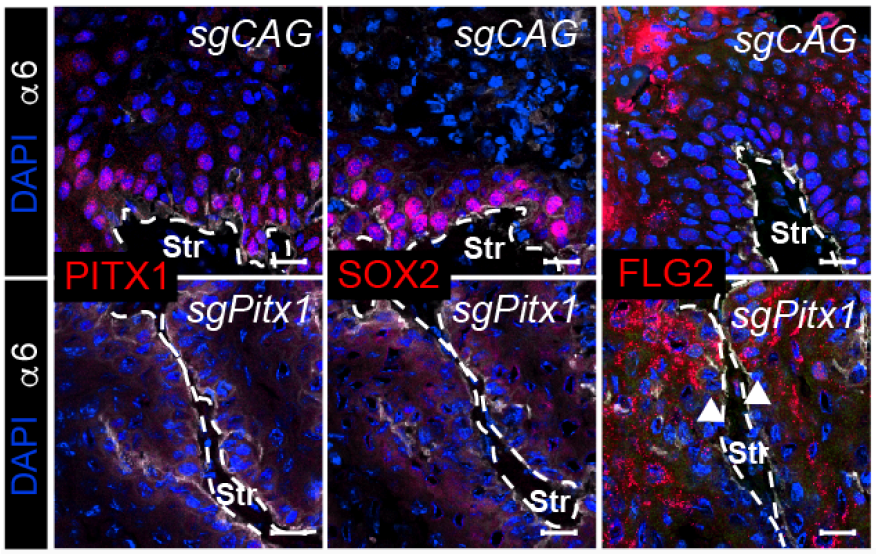

Figure 22: Confocal microscopy for Dox inducible Pitx1 CRISPR-i mediated Pitx1 deletion .It was stained for Pitx1, Sox2 and Flg2. Staining show decreased levels of Sox2 and increased Flg2 expression after Dox inducible Pitx1 CRISPR-i mediated Pitx1 deletion. α6 integrin staining in white, shoes the boundary between the tumor epithelium and the tumor stroma (Str). sgRNAs targeting the CAG promotor were used as a control. Scale bars are 50μm.

There was a great reduction of Pitx1 expression and also Sox2 expression was downregulated. In contrast, Flg2 expression was upregulated, which suggests that the tumors were more differentiated. No just the tumor architecture, but also the tumor growth itself was examined. Before Dox induction, growth of controls (CAG) and Pitx1 interference (O3) tumors was similar (Figure 23). But, a few days after Dox induction, Pitx1 interference tumors start to show a significant reduction in growth rate.

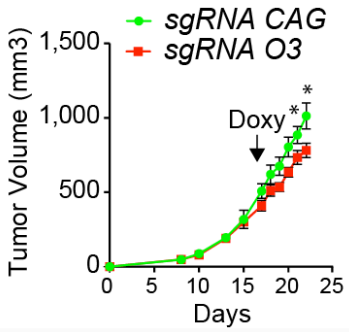

Figure 23:Transduced TPCs with Dox inducible Pitx1 KD. Once tumors were fully established, inhibition was induced and changes in tumor growth rate were measured over time. Inducible Pitx1 KD (sgRNA O3) significantly weakened SCC growth compared to the CAG control.

This data suggests that Pitx1 is not only important to tumor formation, but also for SCC maintenance and tumor growth in addition.

Discussion

It has been suggested that the long-term maintenance of normal tissues and tumors depends on shared mechanisms controlling cell proliferation, self-renewal and survival, even though mutations in proto-oncogenes and tumor suppressors derail homeostasis to support critical hallmarks of cancer (Hanahan and Weinberg, 2000). However, global comparisons of tumor propagating SCC cells and normal skin epithelial stem and progenitor cells challenge this classic perception of tumorigeneses. A broad spectrum of mutations in proto-oncogenes and tumor suppressor genes that is similar to what has been reported in cancers have been identified in normal skin mutational analysis (Martincorena et al., 2015). Furthermore, normal stem cell activities effectively correct oncogene driven aberrant growths to sustain tissue homeostasis by means that are still to be defined (Brown et al., 2017). These observations provide further support for the notion that tumor formation is a rather inefficient process that depends on the dysregulation of multiple cellular processes (Tomasetti and Vogelstein, 2015), and transcriptional changes and epigenetic alterations may be required in addition to mutations in proto-oncogenes and tumor suppressors (Suva et al., 2013). Indeed, differential gene expression analyses uncovered transcriptional signatures that distinguish tumorigenic from normal skin epithelial stem and progenitor cells (Schober and Fuchs, 2011). Despite these striking discoveries, it was still unknown how sequence specific transcription factors elicit transcriptional changes to enable long-term self-renewal and clonal expansion of tumor propagating SCC cells.

We discovered PITX1, a TF that becomes de novo expressed at SCC initiation, as a pivotal regulator of squamous carcinogenesis and functional TPC marker in mouse and human. Although PITX1 is not expressed in normal skin epithelium, it is robustly detected in TPCs and lost as soon as they commit to differentiate into SCC cells without proliferative potential. PITX1 function is critical for the proliferation and survival of TPCs, while its decline prevents further proliferation as squamous differentiation ensues. Similar to SCCs, increased PITX1 expression has been observed in Kras mutant colorectal cancers (Watanabe et al., 2011). We found that the most central circuit comprises multi–input motifs in the tumor specific gene regulatory enhancers of the Pitx1, Sox2, Trp63 and Klf4 genes, which are

collectively controlled by their own gene products in order to establish auto-regulatory circuits. Our data suggest that the association of PITX1, SOX2 and TRP63 with their own enhancers establishes a positive feed forward circuit that sustains their transcription, while their binding to Klf4 regulatory enhancers prevents its expression and the commitment to squamous differentiation. Conversely, reduced PITX1, SOX2 or TRP63 activity enables increased Klf4 transcription, allowing KLF4 protein to bind to Pitx1, Sox2 and Trp63 regulatory elements to intercept their transcription.

A feed forward circuit is also responsible for embryonic stem cell (ESC) self-renewal (Boyer et al., 2005; Yang et al., 2017; Young, 2011) and indeed, tumors are often viewed as tissue regression to a less differentiated state. SOX2 partners with PITX1 and TRP63 to govern gene transcription in TPCs, while its ESC function is determined by Oct4 and Nanog, two transcription factors that are not detected in SCC TPCs (Schober and Fuchs, 2011; Watanabe et al., 2011).

Our data provide a fresh framework, upon which the molecular events leading to tumor formation and maintenance are structured. A detailed understanding of these tumor specific transcriptional networks may provide new opportunities towards the development of novel therapies that target stemness within these cancers (Kreso and Dick, 2014).

References

Al-Barwari, S.E., and Potten, C.S. (1979). A cell kinetic model to explain the time of appearance of skin reaction after X-rays or ultraviolet light irradiation. Cell Tissue Kinet *12*, 281–289.

Alam, M., and Ratner, D. (2001). Cutaneous squamous-cell carcinoma. N. Engl. J. Med. *344*, 975–983.

Argyris, T. (1976). Kinetics of epidermal production during epidermal regeneration following abrasion in mice. Am. J. Pathol. *83*, 329–340.

Arnold, K., Sarkar, A., Yram, M.A., Polo, J.M., Bronson, R., Sengupta, S., Seandel, M., Geijsen, N., and Hochedlinger, K. (2011). Sox2+ Adult Stem and Progenitor Cells Are Important for Tissue Regeneration and Survival of Mice. Cell Stem Cell *9*, 317–329.

Benitah, S.A., and Frye, M. (2012). Stem cells in ectodermal development. J. Mol. Med. *90*, 783–790.

Blanpain, C., and Fuchs, E. (2009). Epidermal homeostasis: a balancing act of stem cells in the skin. Nat. Rev. Mol. Cell Biol. *10*, 207–217.

Botchkarev, V.A., and Flores, E.R. (2014). p53/p63/p73 in the epidermis in health and disease. Cold Spring Harb Perspect Med *4*, a015248–a015248.

Boumahdi, S., Driessens, G., Lapouge, G., Rorive, S., Nassar, D., Le Mercier, M., Delatte, B., Caauwe, A., Lenglez, S., Nkusi, E., et al. (2014). SOX2 controls tumour initiation and cancer stem-cell functions in squamous-cell carcinoma. Nature *511*, 246–250.

Boyer, L.A., Lee, T.I., Cole, M.F., Johnstone, S.E., Levine, S.S., Zucker, J.P., Guenther, M.G., Kumar, R.M., Murray, H.L., Jenner, R.G., et al. (2005). Core transcriptional regulatory circuitry in human embryonic stem cells. Cell *122*, 947–956.

Brown, K., Strathdee, D., Bryson, S., Lambie, W., and Balmain, A. (1998). The malignant capacity of skin tumours induced by expression of a mutant H-ras transgene depends on the cell type targeted. Curr. Biol. *8*, 516–524.

Brown, S., Pineda, C.M., Xin, T., Boucher, J., Suozzi, K.C., Park, S., Matte-Martone, C., Gonzalez, D.G., Rytlewski, J., Beronja, S., et al. (2017). Correction of aberrant growth preserves tissue homeostasis. Nature Publishing Group *548*, 334–337.

Charpentier, E., and Doudna, J.A. (2013). Biotechnology: Rewriting a genome. Nature Publishing Group *495*, 50–51.

Clarke, M.F., Dick, J.E., Dirks, P.B., Eaves, C.J., Jamieson, C.H.M., Jones, D.L., Visvader, J., Weissman, I.L., and Wahl, G.M. (2006). Cancer Stem Cells—

Perspectives on Current Status and Future Directions: AACR Workshop on Cancer Stem Cells. Cancer Res. *66*, 9339–9344.

Cotsarelis, G., Sun, T.T., and Lavker, R.M. (1990). Label-retaining cells reside in the bulge area of pilosebaceous unit: implications for follicular stem cells, hair cycle, and skin carcinogenesis. Cell *61*, 1329–1337.

Deltcheva, E., Chylinski, K., Sharma, C.M., Gonzales, K., Chao, Y., Pirzada, Z.A., Eckert, M.R., Vogel, J., and Charpentier, E. (2011). CRISPR RNA maturation by trans-encoded small RNA and host factor RNase III. Nature Publishing Group *471*, 602–607.

Dominguez, A.A., Lim, W.A., and Qi, L.S. (2015). Beyond editing: repurposing CRISPR–Cas9 for precision genome regulation and interrogation. Nat. Rev. Mol. Cell Biol. *17*, 5–15.

Driessens, G., Beck, B., Caauwe, A., Simons, B.D., and Blanpain, C. (2012). Defining the mode of tumour growth by clonal analysis. Nature Publishing Group *488*, 527–530.

Fuchs, E., Tumbar, T., and Guasch, G. (2004). Socializing with the neighbors: stem cells and their niche. Cell *116*, 769–778.

Gilbert, L.A., Larson, M.H., Morsut, L., Liu, Z., Brar, G.A., Torres, S.E., Stern-Ginossar, N., Brandman, O., Whitehead, E.H., Doudna, J.A., et al. (2013). CRISPR-mediated modular RNA-guided regulation of transcription in eukaryotes. Cell *154*, 442–451.

Greenhalgh, D.A., Rothnagel, J.A., Quintanilla, M.I., Orengo, C.C., Gagne, T.A., Bundman, D.S., Longley, M.A., and Roop, D.R. (1993). Induction of epidermal hyperplasia, hyperkeratosis, and papillomas in transgenic mice by a targeted v-Ha-ras oncogene. Mol. Carcinog. *7*, 99–110.

Guasch, G., Schober, M., Pasolli, H.A., Conn, E.B., Polak, L., and Fuchs, E. (2007). Loss of TGFβ Signaling Destabilizes Homeostasis and Promotes Squamous Cell Carcinomas in Stratified Epithelia. Cancer Cell *12*, 313–327.

Hanahan, D., and Weinberg, R.A. (2000). The Hallmarks of Cancer. Cell *100*, 57–70.

Hsu, P.D., Lander, E.S., and Zhang, F. (2014). Development and applications of CRISPR-Cas9 for genome engineering. Cell *157*, 1262–1278.

Ito, M., Liu, Y., Yang, Z., Nguyen, J., Liang, F., Morris, R.J., and Cotsarelis, G. (2005). Stem cells in the hair follicle bulge contribute to wound repair but not to homeostasis of the epidermis. Nat. Med. *11*, 1351–1354.

Ito, M., Yang, Z., Andl, T., Cui, C., Kim, N., Millar, S.E., and Cotsarelis, G. (2007). Wnt-dependent de novo hair follicle regeneration in adult mouse skin after wounding. Nature *447*, 316–320.

Jaks, V., Kasper, M., and Toftgård, R. (2010). The hair follicle-a stem cell zoo. Exp. Cell Res. *316*, 1422–1428.

Jensen, K.B., Collins, C.A., Nascimento, E., Tan, D.W., Frye, M., Itami, S., and Watt, F.M. (2009). Lrig1 expression defines a distinct multipotent stem cell population in mammalian epidermis. Cell Stem Cell *4*, 427–439.

Jinek, M., Chylinski, K., Fonfara, I., Hauer, M., Doudna, J.A., and Charpentier, E. (2012). A programmable dual-RNA-guided DNA endonuclease in adaptive bacterial immunity. Science *337*, 816–821.

Jones, P.H., Simons, B.D., and Watt, F.M. (2007). Sic transit gloria: farewell to the epidermal transit amplifying cell? Cell Stem Cell *1*, 371–381.

Kearns, N.A., Genga, R.M.J., Enuameh, M.S., Garber, M., Wolfe, S.A., and Maehr, R. (2014). Cas9 effector-mediated regulation of transcription and differentiation in human pluripotent stem cells. Development *141*, 219–223.

Kreso, A., and Dick, J.E. (2014). Evolution of the cancer stem cell model. Cell Stem Cell *14*, 275–291.

Lapouge, G., Youssef, K.K., Vokaer, B., Achouri, Y., Michaux, C., Sotiropoulou, P.A., and Blanpain, C. (2011). Identifying the cellular origin of squamous skin tumors. Proceedings of the National Academy of Sciences *108*, 7431–7436.

Lapouge, G., Beck, B., Nassar, D., Dubois, C., Dekoninck, S., and Blanpain, C. (2012). Skin squamous cell carcinoma propagating cells increase with tumour progression and invasiveness. The EMBO Journal *31*, 4563–4575.

Larson, M.H., Gilbert, L.A., Wang, X., Lim, W.A., Weissman, J.S., and Qi, L.S. (2013). CRISPR interference (CRISPRi) for sequence-specific control of gene expression. Nat Protoc *8*, 2180–2196.

Latil, M., Nassar, D., Beck, B., Boumahdi, S., Wang, L., Brisebarre, A., Dubois, C., Nkusi, E., Lenglez, S., Checinska, A., et al. (2016). Cell-Type-Specific Chromatin States Differentially Prime Squamous Cell Carcinoma Tumor-Initiating Cells for Epithelial to Mesenchymal Transition. Stem Cell 1–35.

Lien, W.-H., Guo, X., Polak, L., Lawton, L.N., Young, R.A., Zheng, D., and Fuchs, E. (2011). Genome-wide Maps of Histone Modifications Unwind In Vivo Chromatin States of the Hair Follicle Lineage. Cell Stem Cell *9*, 219–232.

Limat, A., and Noser, F.K. (1986). Serial cultivation of single keratinocytes from the outer root sheath of human scalp hair follicles. J. Invest. Dermatol. *87*, 485–488.

Mali, P., Aach, J., Stranges, P.B., Esvelt, K.M., Moosburner, M., Kosuri, S., Yang, L., and Church, G.M. (2013). CAS9 transcriptional activators for target specificity screening and paired nickases for cooperative genome engineering. Nat. Biotechnol. *31*, 833–838.

Martincorena, I., Roshan, A., Gerstung, M., Ellis, P., Van Loo, P., McLaren, S., Wedge, D.C., Fullam, A., Alexandrov, L.B., Tubio, J.M., et al. (2015). Tumor evolution. High burden and pervasive positive selection of somatic mutations in normal human skin. Science *348*, 880–886.

Mills, A.A., Zheng, B., Wang, X.J., Vogel, H., Roop, D.R., and Bradley, A. (1999). p63 is a p53 homologue required for limb and epidermal morphogenesis. Nature *398*, 708–713.

Owens, D.M., and Watt, F.M. (2003). Contribution of stem cells and differentiated cells to epidermal tumours. Nat. Rev. Cancer *3*, 444–451.

Perez-Losada, J., and Balmain, A. (2003). Stem-cell hierarchy in skin cancer. Nat. Rev. Cancer *3*, 434–443.

Perez-Pinera, P., Kocak, D.D., Vockley, C.M., Adler, A.F., Kabadi, A.M., Polstein, L.R., Thakore, P.I., Glass, K.A., Ousterout, D.G., Leong, K.W., et al. (2013). RNA-guided gene activation by CRISPR-Cas9–based transcription factors. Nature Methods *10*, 973–976.

Pierce, G.B., and Wallace, C. (1971). Differentiation of malignant to benign cells. Cancer Res. *31*, 127–134.

Qi, L.S., Larson, M.H., Gilbert, L.A., Doudna, J.A., Weissman, J.S., Arkin, A.P., and Lim, W.A. (2013). Repurposing CRISPR as an RNA-Guided Platform for Sequence-Specific Control of Gene Expression. Cell *152*, 1173–1183.

Rheinwatd, J.G., and Green, H. (1975). Seria cultivation of strains of human epidemal keratinocytes: the formation keratinizin colonies from single cell is. Cell *6*, 331–343.

Rochat, A., Kobayashi, K., and Barrandon, Y. (1994). Location of stem cells of human hair follicles by clonal analysis. Cell *76*, 1063–1073.

Schober, M., and Fuchs, E. (2011). Tumor-initiating stem cells of squamous cell carcinomas and their control by TGF-β and integrin/focal adhesion kinase (FAK) signaling. Proc. Natl. Acad. Sci. U.S.a. *108*, 10544–10549.

Siegle, J.M., Basin, A., Sastre-Perona, A., Yonekubo, Y., Brown, J., Sennett, R., Rendl, M., Tsirigos, A., Carucci, J.A., and Schober, M. (2014). SOX2 is a cancer-specific regulator of tumour initiating potential in cutaneous squamous cell carcinoma. Nature Communications *5*, 1–12.

Suva, M.L., Riggi, N., and Bernstein, B.E. (2013). Epigenetic Reprogramming in Cancer. Science *339*, 1567–1570.

Tomasetti, C., and Vogelstein, B. (2015). Cancer etiology. Variation in cancer risk among tissues can be explained by the number of stem cell divisions. Science *347*, 78–81.

Truong, A.B., and Khavari, P.A. (2007). Control of keratinocyte proliferation and differentiation by p63. Cell Cycle *6*, 295–299.

Watanabe, T., Kobunai, T., Yamamoto, Y., Matsuda, K., Ishihara, S., Nozawa, K., Iinuma, H., Ikeuchi, H., and Eshima, K. (2011). Differential gene expression signatures between colorectal cancers with and without KRAS mutations: crosstalk between the KRAS pathway and other signalling pathways. Eur. J. Cancer *47*, 1946–1954.

Watt, F.M., and Hogan, B.L. (2000). Out of Eden: stem cells and their niches. Science *287*, 1427–1430.

White, A.C., Tran, K., Khuu, J., Dang, C., Cui, Y., Binder, S.W., and Lowry, W.E. (2011). Defining the origins of Ras/p53-mediated squamous cell carcinoma. Proc. Natl. Acad. Sci. U.S.a. *108*, 7425–7430.

Yang, H., Schramek, D., Adam, R.C., Keyes, B.E., Wang, P., Zheng, D., and Fuchs, E. (2015). ETS family transcriptional regulators drive chromatin dynamics and malignancy in squamous cell carcinomas. Elife *4*, e10870.

Yang, Y., Liu, B., Xu, J., Wang, J., Wu, J., Shi, C., Xu, Y., Dong, J., Wang, C., Lai, W., et al. (2017). Derivation of Pluripotent Stem Cells with In Vivo Embryonic and Extraembryonic Potency. Cell *169*, 243–257.e25.

Young, R.A. (2011). Control of the Embryonic Stem Cell State. Cell *144*, 940–954.